



## THE INFLUENCE OF FLUID PROPERTIES AND DUCT GEOMETRY ON GAS-LIQUID FLOW PATTERNS

**Fernando Augusto Alves Mendes**

**Oscar Maurício Hernandez Rodriguez**

Department of Mechanical Engineering, São Carlos School of Engineering, University of São Paulo (USP)

Av. Trabalhador São Carlense, 400, 13566-970, São Carlos-SP, Brazil

[faamendes@gmail.com](mailto:faamendes@gmail.com) and [oscarmhr@sc.usp.br](mailto:oscarmhr@sc.usp.br)

**Valdir Estevam**

PETROBRAS/E&P-ENGP/TPP/EE

[vestevam@petrobras.com.br](mailto:vestevam@petrobras.com.br)

**Divonsir Lopes**

PETROBRAS/UN-RIO/ENGP/EE

[divonsir@petrobras.com.br](mailto:divonsir@petrobras.com.br)

**Abstract.** *Two-phase flow is common in the petroleum industry, especially in offshore directional wells and pipelines. The main purpose of this study is to investigate the influence of fluid properties and duct geometry on the transition of flow patterns and pressure drop in ducts compatible with the dimensions used by the oil industry. New experimental data collected in the Thermal-Fluids Engineering laboratory of the Engineering School of São Carlos of University of São Paulo (LETeF) and data obtained from literature were used in the present study. The experimental data was collected in an apparatus especially designed and built for this purpose which consists of an inclinable test section, 0 to 90 degrees, with inner and outer diameters of 75 mm and 111 mm, respectively, hence the annular channel possessing an 18 mm gap. The total length of the test section was of 10.5 m. Air, water and oil at near atmospheric pressure constituted the gas and liquid phases. The air, water and oil superficial velocities were in the range of 0.01–10 m/s, 0.008–0.8 m/s and 0.003–0.1 m/s, respectively. Comparisons between data and flow-pattern maps available in the literature for annular-duct flow allowed for the discrimination of regions and flow situations for which improvements of the transition modelling are required.*

**Keywords:** *flow patterns, gas-liquid flow, annular duct.*

### 1. INTRODUCTION

The multiphase flow in annular duct can be found frequently in the oil industry, for instance in directional wells that are completed with a sand screen and in the concentric or eccentric annuli in oil/gas well drilling. Also, gas-liquid flow in annular ducts is found in the petroleum industry associated with gravitational gas separators that are applied with the Electrical-Submersible-Pump (ESP) technique for oil production. However, the available information about the phenomenology of this type of flow is scanty.

(Kelessidis and Dukler, 1989) presented a study on upward-vertical two-phase flow in an annular duct. The authors traced flow-patterns maps and established the transitions of flow patterns experimentally. (Hasan and Kabir, 1992) proposed a phenomenological model for transitions in upward vertical and inclined annular duct flow and used data from the literature to validate the model. (Caetano et al., 1992) carried out an experimental and theoretical study of the effect of eccentricity in an upward-vertical two-phase annular-duct flow. (Hasan and Kabir, 1992) studied the influence of inclination on flow patterns, however the model was validated only with data of upward-vertical flow. (Wongwises and Pipathattakul, 2006) and (Ekberg et al., 1999) show results for horizontal two-phase annular-duct flow. In the former the authors were looking for the effect of slope on flow patterns, while in the latter the air-water flow patterns were classified and compared in two different sections test. In both studies they used small tubes (annular channel gap of about 1 mm), which is not compatible with the dimensions used by the oil industry. Furthermore, those authors have not proposed any model for flow pattern transition. (Blanco et al., 2008) conducted a thorough review on gas-liquid flow patterns in annular duct and proposed flow-patterns maps for horizontal and vertical inclinations. However, those authors didn't validate the proposed methodology with data related to dimensions similar to those found in the oil industry, because of the lack of available data in the literature. Therefore, one of the main purposes of this study is to expand the existing experimental database on gas-liquid flow in annular ducts.

Visualization and analysis of high-frequency pressure-signature signals in time and frequency domains are used for flow pattern characterization in the present work. The flow-patterns maps obtained in this work were compared with literature data.

## 2. EXPERIMENTAL SETUP AND PROCEDURE

### 2.1 Experimental setup

The gas-liquid flow experimental data were obtained in the multiphase-flow loop of the Thermal-Fluids Engineering Laboratory (NETeF) of the Engineering School of Sao Carlos, University of Sao Paulo (USP), Fig. 1. The test section (TS) has an annular geometry and is made of borosilicate glass. It has 10.5 m of length and is sustained by an inclinable truss beam capable of going from horizontal to 90 degrees of inclination. There is a flow development section of 1.5 m and 111 mm of internal diameter before the annular duct of 7.5 m and 111 mm of outside diameter ( $D_o$ ) and 75 mm of internal diameter ( $D_i$ ), Fig. 2. A pipe section, identical to the development section, was positioned after the annular test section.

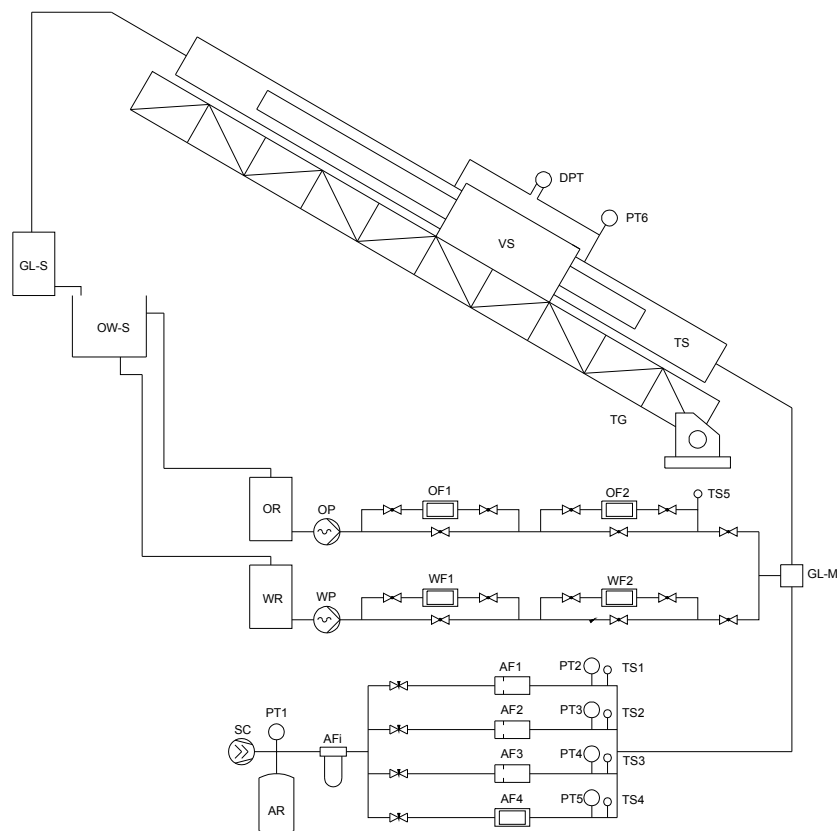


Figure 1. Schematic of the multiphase-flow loop of the Thermal-Fluids Engineering Laboratory (NETeF).

The air was supplied by a Worthington screw compressor of 50 kW model ROLLAIR 40 (SC), whose flow control is done by needle valves positioned before the flow meters. Three orifice plates (AF1, AF2, AF3) and a positive displacement flow meter model Oval Gal 50 (AF4) were used for measuring the air flow. The tap water used in test is pumped from a water tank (WR) by a Weatherford progressive cavity helical pump of 11kW model WHT (WP). To measure the water flow it is used a Badger Meter positive displacement flow meter OGT (WF1) and an Oval vortex water flow meter model EX Delta. The oil is pumped by a Weatherford progressive cavity helical pump of 11kW model WHT (OP). Two Oval positive displacement flow meters are used to measure the oil flow: MIII (OF1) and Flowpet EG (OF2). The gas-liquid mixture is formed in the gas-liquid mixer (GL-M), it is separated in the gas-liquid separator (GL-S) and the air is vented to the atmosphere. The liquid returned by gravity to tank (WR) or (OR). Novus pressure transducers TP-150 with range of 0-5 bar, accuracy 0,5% FS (PT2, PT3, PT4, PT5, PT6) were used to measure pressure and IOPE temperature sensor model TW-TC/2 (TS1, TS2, TS3, TS4, TS5), range -20 – 140 °C and accuracy  $\pm 0,5$  °C were used to measure temperature. Table 1 summarizes the main instruments used in this study.

A Validayne differential pressure transducer, model DP-15 (DPT), was used to acquire the two-phase flow pressure signature. At the entrance of the acquisition system it was installed a low-pass filter of 20 Hz to eliminate the signal noise of the pressure transducer. The remote control and acquisition system consisted of a PC equipped with a National Instruments acquisition board model PCI-6224. The water pump was controlled with the assistance of a CAM system. The inclination angle of the test section (TS) is measured with a Bosh angle meter DNM 60L, accuracy  $\pm 0,2^\circ$ .

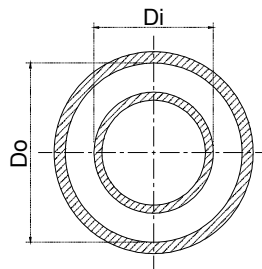


Figure 2. Schematic of the annular-duct test section.

Table 1. Measurement instruments.

Flow meter	Range at 101325 Pa and 273,15 K (l/min)	Accuracy
AF1	57 – 262	±1% RD
AF2	172 – 794	±1% RD
AF3	524 – 2400	±1% RD
AF4	1.2 – 20	+1% RD
OF1	0.05 – 8	±1% RD
OF2	2.5 – 106	±1% RD
WF1	1 – 35	±1% RD
WF2	30 – 1300	±1% RD

## 2.2 Fluids characteristics

The experiments were carried out at oil and water temperatures around 20°C, the ambient temperature around 25°C

### 2.2.1 Water

The water used in the experiments has density of 988 kg/m<sup>3</sup>, viscosity of 0,001 Pa.s at temperature of 20°C. The air-water superficial tension was of 0,072 N/m.

### 2.2.2 Oil

The oil used had density of 828 kg/m<sup>3</sup> and viscosity of 0.3 Pa.s at 20°C. The oil-water interfacial tension was 0,034 N/m and air-oil superficial tension was 0,054 N/m. The oil-water contact angle with the borosilicate glass was 29° (hydrophilic-oilphobic).

The viscosity were measured with a rheometer Brookfield™, model LVDV-III+ with the rotor SC4-18. The interfacial tension and contact angle were measured with an optical tensiometer of KSV™, model CAM 200.

## 2.3 Experimental procedure

The test section (TS) was set to the desired angle. The liquid superficial velocity was established by the pump control system using a PID controller implemented in LabView™ platform. The air injection was controlled manually through the needle valves. After five minutes, which was enough time to ensure steady state, the signal provided by the pressure transducer was saved for a period of 60 s. The flow-pattern transition boundaries were determined a posteriori by visual observations (subjective technique) and the signal analysis (objective technique), based on the Fourier transform (FFT) and the Probability density function (PDF) of the pressure-signature signal.

## 3. RESULTS AND DISCUSSION

### 3.1 Objective analysis

The Validyne differential pressure transducer was mounted with diaphragm 32 (pressure range of -14 to 14 kPa) for identify flow patterns. Data were acquired at a rate of 5 kHz, with an accuracy of 0.5% FS and analyzed by a homemade program implemented in LabView™.

### 3.1.1 Air-water flow

Figures 3-6 illustrates the time and frequency domain signals in upward-vertical air-water bubble, slug, churn and annular flow, respectively. The pressure signature related to bubble flow (Fig. 3a) is smoother than that of slug or churn flow. In addition, the PSD indicates the presence of high frequency oscillations around 10 Hz only for bubble flow (Fig. 3b). In churn flow the signal is characterized by high amplitudes due to the intermittence between upward and downward liquid flow (Fig. 5a). It is worth noting that the signal related to churn flow can reach values that slightly overcome the value of the hydrostatic pressure of the equivalent water column (10.4 kPa), which is likely due to high frictional pressure loss and high void fraction. On the other hand, in annular flow the interfacial shear stress stabilizes the flow, because of the very high gas superficial velocity and void fraction. This statement becomes evident when one looks at Fig. 6a. The signal has low amplitudes in time and the time-averaged pressure value is significantly higher to the hydrostatic pressure of the equivalent water column (10.4 kPa).

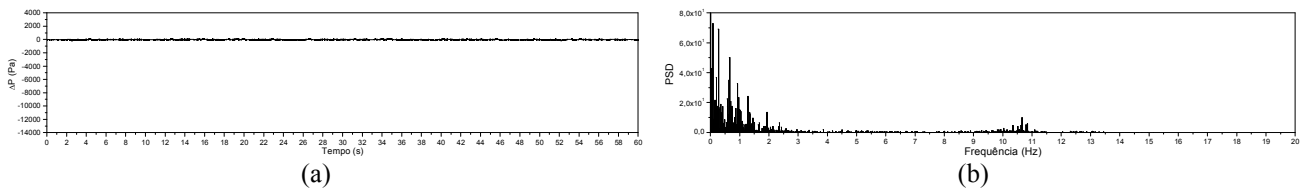


Figure 3. Bubble flow ( $J_A=0.01$  m/s;  $J_W=0.1$  m/s). a) Signal and b) PSD.

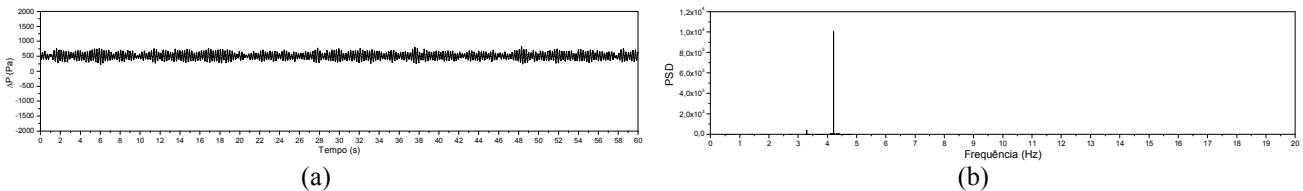


Figure 3. Dispersed Bubble flow ( $J_A=0.01$  m/s;  $J_W=0.80$  m/s). a) Signal and b) PSD.

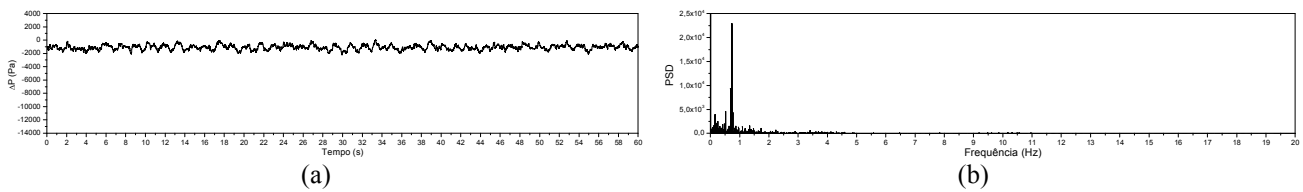


Figure 4. Slug flow ( $J_A=0.1$  m/s;  $J_W=0.01$  m/s). a) Signal and b) PSD.

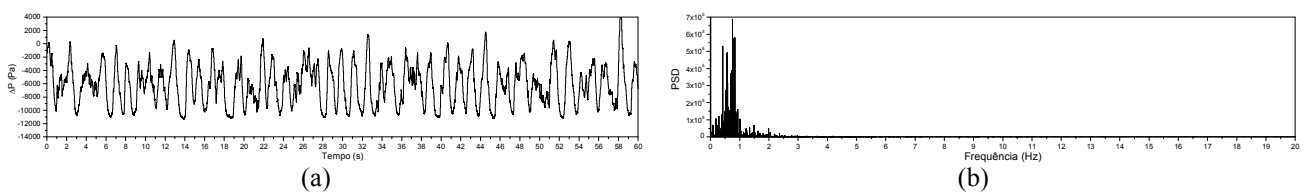


Figure 5. Churn flow ( $J_A=1.6$  m/s;  $J_W=0.02$  m/s). a) Signal and b) PSD.

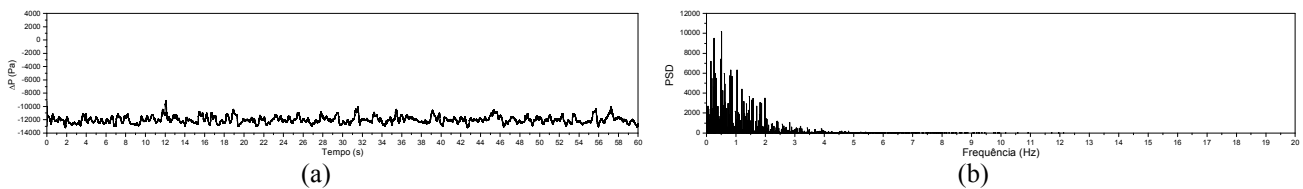


Figure 6. Annular flow ( $J_A=7.16$  m/s;  $J_W=0.01$  m/s). a) Signal and b) PSD.

### 3.1.2 Air-oil flow

The Figs 7-10 illustrate the pressure signatures and related PSD graphs related to vertical air-oil bubble, slug, churn and annular flow, respectively. The time signal of bubble flow is smooth when compared to the signals of slug and churn flow. The behavior of the signal in air-oil bubble flow is similar to that observed in air-water bubble flow. As in air-water churn flow (Fig. 5a), the signal of air-oil churn flow is characterized by large amplitudes (Fig. 24a). The signal related to air-oil annular flow, Fig. 10, has similar characteristics in comparison with that of air-water annular flow, Fig. 6.

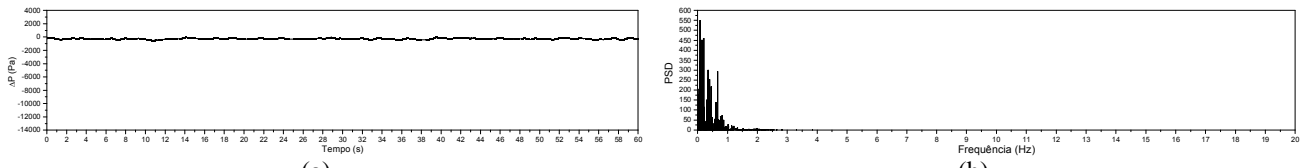


Figure 7. Bubble flow ( $J_A=0.014$  m/s;  $J_O=0.097$  m/s). a) Signal and b) PSD.

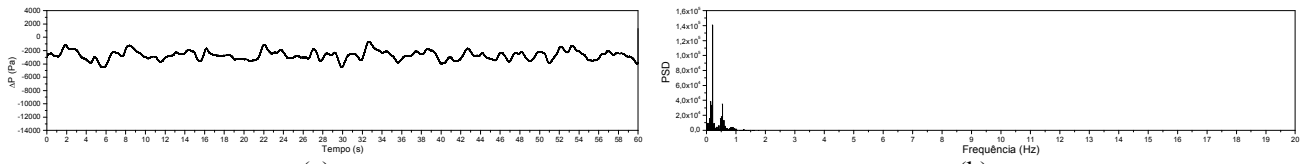


Figure 8. Slug flow ( $J_A=0.125$  m/s;  $J_O=0.019$  m/s). a) Signal and b) PSD.

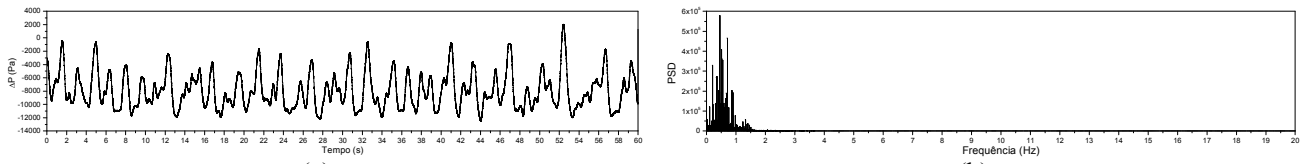


Figure 9. Churn flow ( $J_A=2.10$  m/s;  $J_O=0.037$  m/s). a) Signal and b) PSD.

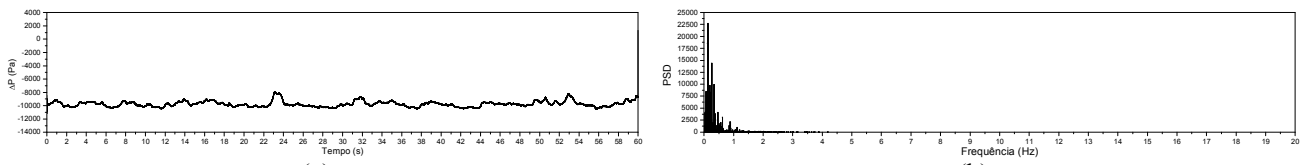


Figure 10. Annular flow ( $J_A = 6.90$  m/s;  $J_O = 0,004$  m/s); a) Sinal and b) PSD.

### 3.2 Flow patterns maps

The Figs 11 and 12 illustrate the flow-pattern maps for large annular duct obtained experimentally with the test section inclined at 45° and 90°, respectively. The gas flow rate was normalized according to the normal temperature and pressure (NTP). In both situations the dispersed bubble flow occurs for liquid superficial velocities above 0.6 m/s.

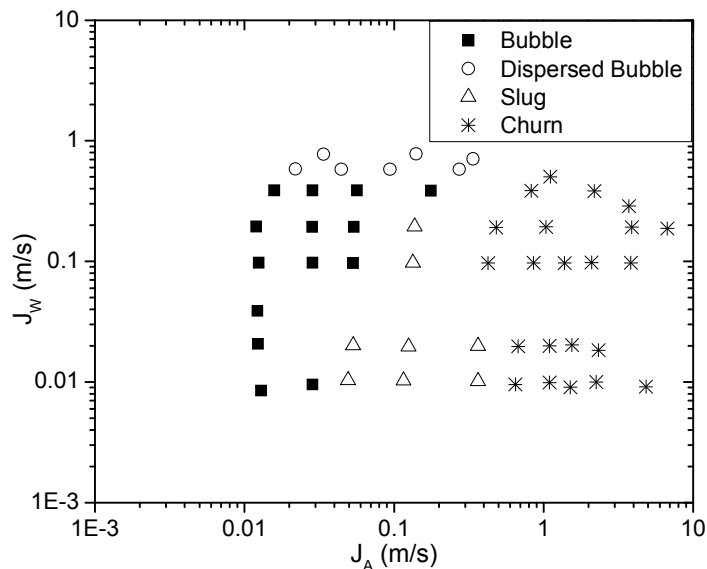


Figure 11. Air–water annular-duct flow-pattern map at +45°.

With the test section at  $45^\circ$  and liquid superficial velocity above 0.01 m/s, the bubble flow isn't observed for gas superficial velocities above of 0.03 m/s. With an inclination of  $90^\circ$  and the same liquid superficial velocity, the bubble flow was observed for gas superficial velocity below 0.1 m/s. This difference can be explained by the effect of gravitational component that appears in the radial direction of duct for the test section positioned at  $45^\circ$ , accumulating bubbles in the upper part of the duct and, consequently, transition to the pattern slug flow.

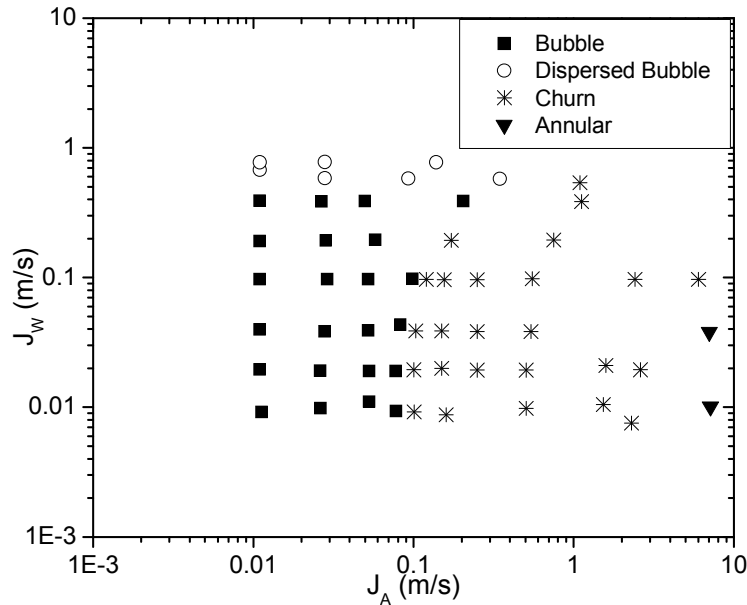


Figure 12. Vertical air–water annular-duct flow-pattern map.

The gravitational effect can explain the absence of annular flow in Fig. 11, it has been observed visually, for high gas superficial velocities and test section inclined at  $45^\circ$ , the accumulation of liquid in the bottom part of the duct followed by a free surface flow.

Figure 13 illustrates the air-water flow-pattern map obtained by (Kelessides and Dukler 1989) to a annular duct with dimensions i.d. 50.8 mm and o.d. 76.2 mm. Figure 14 shows the experimental map obtained by (Caetano et al. 1992) with a annular duct i.d. 42 mm and o.d. 76 mm, both studies were performed vertically.

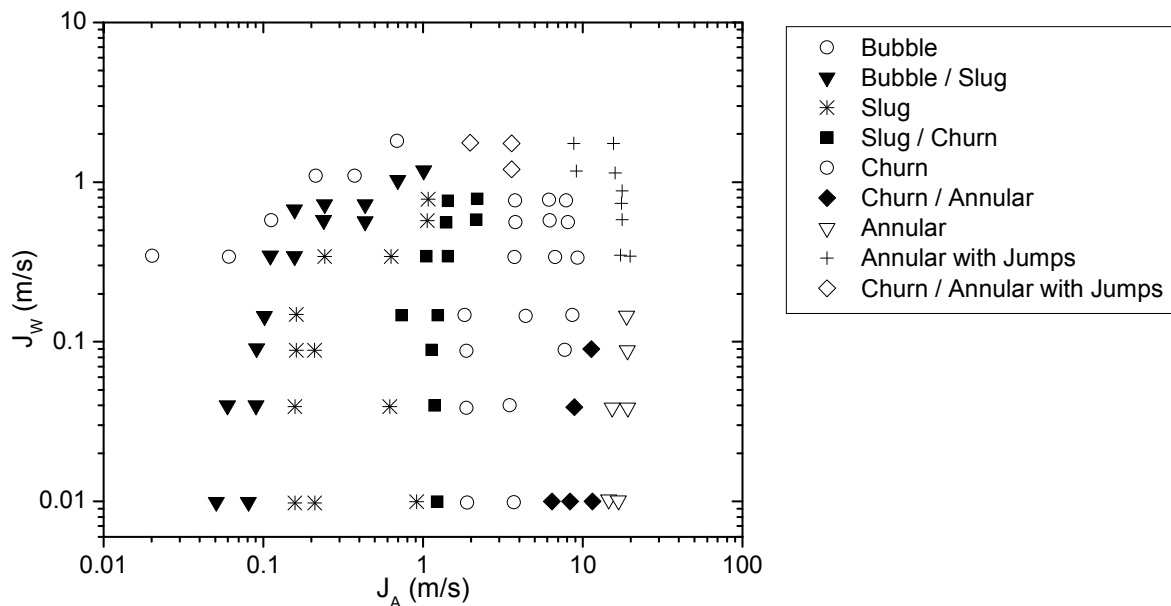


Figure 13. Vertical air–water annular-duct flow-pattern map by (Kelessides and Dukler, 1989).

In the studies of (Kelessides and Dukler, 1989) and (Caetano et al., 1992) the slug flow was observed from a gas superficial velocity of 0.1 m/s whereas in the present study hydrodynamic instabilities prevented the formation of the

Taylor bubbles at 90°. The hydraulic diameter of this work is 36 mm and the work (Caetano et al., 1992) is 34 mm, relatively equal. Therefore, the emergence of hydrodynamic instabilities may be related to size of the duct, which is 150% higher in the present work. It should be noted that (Oddie et al., 1998) conducted a study with a circular duct in the same dimensions used in this study and was not observed the slug flow in vertical flow. In the region where observe the slug flow in duct dimensions smaller, in the present work is the churn flow.

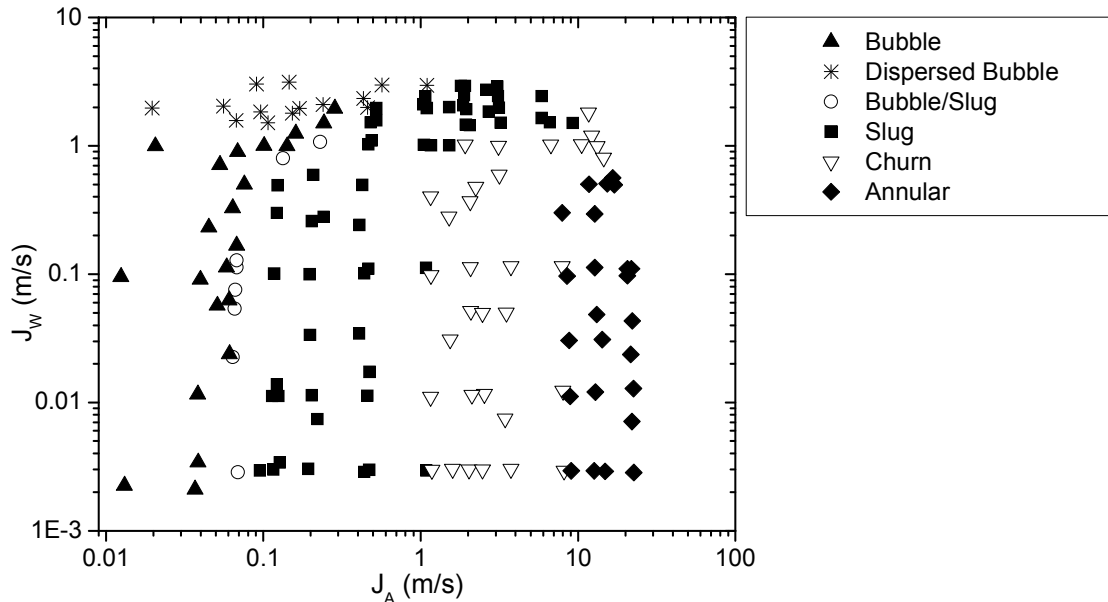


Figure 14. Vertical air–water annular-duct flow-pattern map by (Caetano et al., 1992).

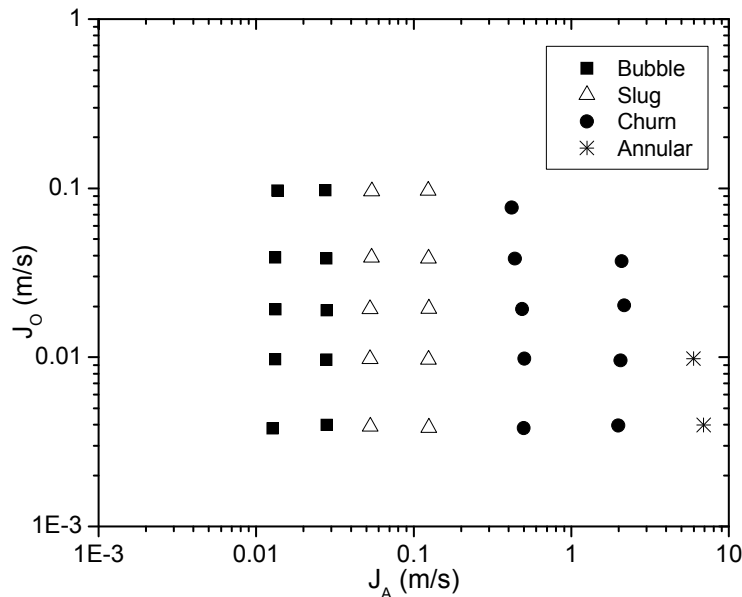


Figure 15. Vertical air–oil annular-duct flow-pattern map.

Stands a big difference between the annular flow region observed in the literature and the region of the same flow observed in this study. For duct smaller the annular flow can be observed from a gas superficial velocity of 10 m/s while in this work it is possible to observe the annular flow for gas superficial velocities of 7 m/s.

The dispersed bubble flow was not observed by (Kelessides and Dukler, 1989) However, this type of flow was observed in work realized by (Caetano et al., 1992), and in this study. (Caetano et al., 1992) observed the dispersed bubble flow from liquid superficial velocities above to 1m/s whereas in this work was observed the dispersed bubble flow for liquid superficial velocity of 0.7 m/s. It is believed that the transition of the bubble flow from dispersed bubbles flow in annular ducts may be associated with diameter hydraulic when compared the works of (Caetano et al., 1992) and (Kelessides and Dukler, 1989). When it is compared the present work with work Caetano reaches the conclusion that the size of the duct is also an important parameter.

F. A. A. Mendes, O. M. H. Rodriguez, V. Estevam, D. Lopes  
The Influence of Fluid Properties and Duct Geometry on Gas-Liquid Flow Patterns

Slug flow was indeed observed in upward-vertical oil-water flow, Fig. 15, differently from what was seen in air-water flow (Fig. 15). It occurred for superficial gas velocities between 0.05 m/s and 0.4 m/s and for superficial liquid velocity below 0.1 m/s. The instabilities, responsible for breaking up the imminent Taylor bubbles in air-water flow, are damped perhaps due to the higher viscosity of oil; besides, less turbulence is expected to take place in the liquid phase in oil-water flow. Finally, in the upward-vertical air-oil flow the annular flow was observed for superficial gas velocities above 6 m/s (Fig. 15), which is similar to what was seen in vertical air-water flow (Fig. 12).

#### 4. CONCLUSIONS

Air-water and air-oil flow patterns for inclined and vertical flow in a large annular duct were identified and characterized in this study. The experimental results were obtained in a 10.5 m length test section of borosilicate glass with inner diameter of 75 mm and outer diameter of 111 mm. The inclinations of the test section were  $+45^\circ$  and  $+90^\circ$  in relation to the horizontal. The ranges of superficial velocities of water, oil and air were 0.008 to 0.8 m/s, 0.003 to 0.1 m/s and 0.01 to 10 m/s, respectively. With it inclined at  $+45^\circ$ , bubbles, slug, churn and dispersed bubbles were observed. The slug flow is observed at gas superficial velocities above 0.05 m/s in both air-oil and air-water flows. The dispersed-bubble flow occurs at liquid superficial velocities above 0.6 m/s at  $+45^\circ$  and vertical. The results help to assess the potentiality of using a simple pressure-signature-based objective technique as a tool for identifying flow-pattern transition boundaries in air-water and air-oil flows at several inclinations in a big annular duct. The dimensions of the ducts and properties of the fluids are parameters that influence the transition boundaries of the flow-patterns maps in vertical annular-duct. Another finding is the clear necessity of developing phenomenological models capable of accurately generate flow-pattern maps for gas-liquid flow in annular ducts with dimensions similar to that used in the petroleum industry.

#### 5. ACKNOWLEDGEMENTS

The present study was financially supported by PETROBRAS, whose guidance and assistance are gratefully acknowledged.

#### 6. REFERENCES

- Blanco, C.P., Albieri, T.F., and Rodriguez, O.M.H., 2008. "Revisão de Modelagem para Transições de Padrão de Escoamento Gás-Líquido em Duto Anular Vertical e Horizontal," In *12th Brazilian Congress of Thermal Engineering and Sciences – ENCIT2008*, Belo Horizonte, Brazil.
- Caetano, E.F., Shoham, O. and Brill, J.P., 1992. "Upward Vertical Two-Phase Flow Through an Annulus---Part I: Single-Phase Friction Factor, Taylor Bubble Rise Velocity, and Flow Pattern Prediction," *Journal of Energy Resources Technology*, Vol. 114, no. 1, pp. 1-13.
- Ekberg, N.P., Ghiaasiaan, S.M., Abdel-Khalik, S.I., Yoda, M. and Jeter, S.M., Aug. 1999. "Gas-liquid two-phase flow in narrow horizontal annuli," *Nuclear Engineering and Design*, Vol. 192, no. 1, pp. 59-80.
- Hasan, A. R. and Kabir, C. S., Mar. 1992. "Two-phase flow in vertical and inclined annuli," *International Journal of Multiphase Flow*, Vol. 18, no. 2, pp. 279-293.
- Kelessidis, V. C. and Dukler, A. E., Apr. 1989. "Modeling flow pattern transitions for upward gas-liquid flow in vertical concentric and eccentric annuli," *International Journal of Multiphase Flow*, Vol. 15, no. 2, pp. 173-191.
- Oddie, G., Shi, H., Durlofsky, L.J., Aziz, K, Pfeffer, B., Holmes, J.A., 2003. "Experimental study of two and three phase flows in large diameter inclined pipes" *International Journal of Multiphase Flow*, Vol. 29, pp. 527-558.
- Wongwises, S., and Pipathattakul, M., Mar 2006. "Flow pattern, pressure drop and void fraction of two-phase gas-liquid flow in an inclined narrow annular channel," *Experimental Thermal and Fluid Science*, Vol. 30, no. 4, pp. 345-354.

#### 7. RESPONSIBILITY NOTICE

The author(s) is (are) the only responsible for the printed material included in this paper.